Molecular Boundary Conditions and Accommodation Coefficient on A Nonequilibrium Liquid Surface

Takaharu Tsuruta, Atsushi Tokunaga and Gyoko Nagayama

Kyushu Institute of Technology, Sensui1-1, Tobata, Kitakyushu 804-8550, Japan

Abstract. The non-equilibrium molecular dynamics (NEMD) simulations have been carried out to obtain new evidence about inverted temperature profiles. We find that the inverted temperature profile occurs due to the excess energy of the reflecting molecules without contradiction to the second law. Therefore, a new definition of the accommodation coefficient for the reflecting molecule is proposed based on the energy of the reflecting molecule under the equilibrium condition. The accommodation coefficient decreases with increasing the mass flux in the vicinity of the liquid surface and this is the reason for the inverted temperature profile. Also, a direct simulation of Monte Carlo (DSMC) method has been performed with applying the molecular boundary condition developed in the non-equilibrium molecular dynamics simulation. An inverted temperature profile is obtained because the energy of the reflecting molecule cannot reach accommodations to that of the equilibrium ones.

Keywords: Accommodation coefficient for reflecting molecule, Nonequilibrium liquid surface, Molecular dynamics

INTRODUCTION

The condensation coefficient plays an important role in the condensation phenomena. In many studies, condensation coefficient has been given unity or a uniform value less than unity without respect to kinetic motion of molecules. However, it was found by Tsuruta et al. that the condensation coefficient depended on the normal component of the incident molecular velocity to the liquid surface[1, 2]. They proposed a new model of the boundary conditions at the liquid-vapor interface under equilibrium conditions. Also, a direct simulation Monte Carlo (DSMC) analysis has been carried out[3] using these boundary conditions in order to clarify the inverted temperature profile, which is known as a paradox of thermodynamics[4]. Other studies using non-equilibrium molecular dynamics have been carried out and the inverted temperature profile also has been confirmed in these results[5, 6]. Some of the researchers have discussed the criteria for the inverted temperature profile based on the irreversible thermodynamics and they pointed that the phenomenon is not in contradiction to the second low[7, 8]. However, the mechanism of the occurrence of the inverted temperature profile is not clarified yet. Recently, we have performed the non-equilibrium molecular dynamics simulation and the results of the inverted temperature profile are discussed from the view point of the irreversible thermodynamics and the kinetic theory. Our results support the occurrence of the inverted temperature profile in the vicinity of the condensing surface under the non-equilibrium condition without any contradiction to the second law. It is found that the inverted temperature profile takes place because the reflected molecules have the excess energy than those in equilibrium state[9].

In this paper, we have carried out molecular dynamics simulation (NEMD) in order to reach a better understanding on the molecular boundary conditions at the non-equilibrium liquid surface. The characteristics of the reflecting molecules are focused on because the kinetic motion of the reflecting molecules plays an important role on the non-equilibrium condensing surface.

MOLECULAR BOUNDARY CONDITIONS

In general, the condensation/evaporation coefficient has been considered to have the uniform value irrespective of kinetic motion of molecules in the discussion. It is found, however, that the condensation probability depends on the surface-normal component of incident velocity. According to molecular dynamics studies (MD), the microscopic

formulation of the condensation coefficient has been given as a function of the molecular incident velocity normal to the surface and the surface temperature[1, 2]:

$$\sigma_c = \alpha\left\{1-\beta\, exp\left(-\frac{mV_z^{\,2}}{2k_BT}\right)\right\} \tag{1}$$

where V_z is the normal component of the molecular velocity to the surface, k_B is the Boltzmann constant, m is the mass of molecule, T is the temperature of the liquid surface and the parameters α and β are constants. According to transition state theory and MD results, it is found that the parameters α and β are relevant to the specific volume of vapor and liquid[10].

The evaporation coefficient in the equilibrium condition is equal to the condensation coefficient because the evaporation flux and the condensation flux have a same value. Since the all leaving molecules from the liquid surface coincide with the Maxwellian velocity distribution in the equilibrium condition, the velocity distribution functions for the evaporating and reflecting molecules can be expressed as follows:

$$f_e = \sigma_c n\left(\frac{m}{2\pi k_BT}\right)^{1/2} exp\left(-\frac{mV^2}{2k_BT}\right) \tag{2}$$

$$f_r = (1-\sigma_c) n\left(\frac{m}{2\pi k_BT}\right)^{1/2} exp\left(-\frac{mV^2}{2k_BT}\right) \tag{3}$$

Therefore, the density functions of velocity distribution, F_e and F_r are obtained by normalizing Eqs. (2) and (3).

$$F_{z,r} = \frac{1-\alpha+\alpha\beta exp\left(-mV_z^{\,2}/(2k_BT)\right)}{1-\alpha+\alpha\beta/2}\times\left(\frac{m}{k_BT}\right)V_z\, exp\left(-\frac{mV_z^{\,2}}{2k_BT}\right) \tag{4}$$

$$F_{z,e} = \frac{1-\beta exp\left(-mV_z^{\,2}/(2k_BT)\right)}{1-\beta/2}\times\left(\frac{m}{k_BT}\right)V_z\, exp\left(-\frac{mV_z^{\,2}}{2k_BT}\right) \tag{5}$$

Equations (1), (4) and (5) give the molecular boundary conditions for the equilibrium liquid surface[11]. These molecular boundary conditions are important in order to understand the heat and mass transport phenomena in the vicinity of the condensing surface.

INVERTED TEMPERATURE PROFILE

Based on kinetic theory, Pao predicted that the temperature gradient in a vapor between two liquids kept at different temperatures could be inverted compared to the applied temperature difference[4]. That is, the heat flux in the vicinity of the condensing surface occurs in the opposite direction of the condensing flow. This phenomenon is generally called "the inverted temperature profile" and has been discussed for years in kinetic theory[7,12-15], molecular simulations[3,5,6,8] and experiments[16,17] to confirm the prediction by Pao. Tsuruta et al.[3] have been carried out DSMC analysis using the boundary conditions shown in Eqs. (1), (4) and (5) at the liquid-vapor interface. Figure 1 shows the temperature profile obtained by DSMC. There is no inverted temperature gradient in the case of α=0.923 and β=0.299 and the dimensionless temperatures at the interface are almost the same around 0.6. However, if the dependency on the molecular velocity is ignored (β=0), the inverted temperature profile occurs even in the same mass transfer rate. For the case of the condensation coefficient is unity (α=1), we can find a clear negative temperature profile in the vicinity of the condensing surface. Therefore, Tsuruta et al. suggest that the inverted temperature profile only occurs in an inadequate molecular boundary condition of the condensation coefficient.

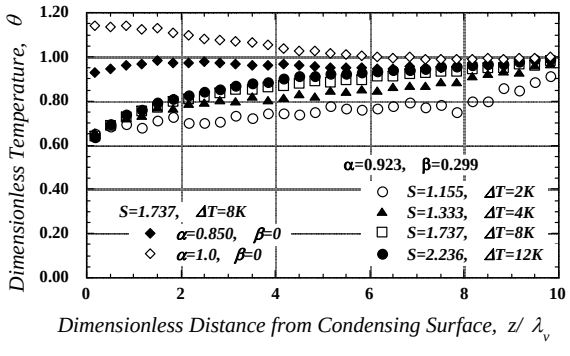

Figure 1 Comparison of temperature profiles for different boundary conditions at the condensing surface (DSMC results for 102K argon surface).

However, the inverted temperature profile has still be confirmed in recent years[5,6], for example, Johannessen and Bedeaux[18] presented numerical solutions in the nonequilibrium Van der Waals square gradient model in order to verify the criterion for the occurrence of the

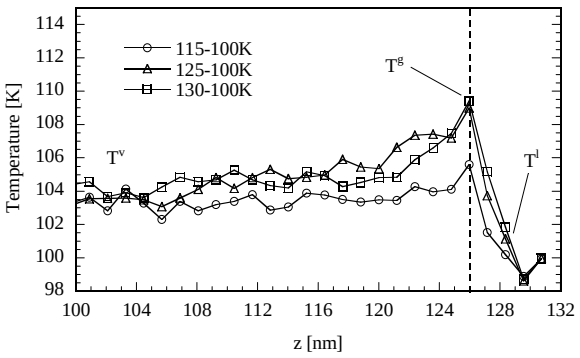

Figure 2 Inverted temperature profiles at condensing surface (NEMD results).

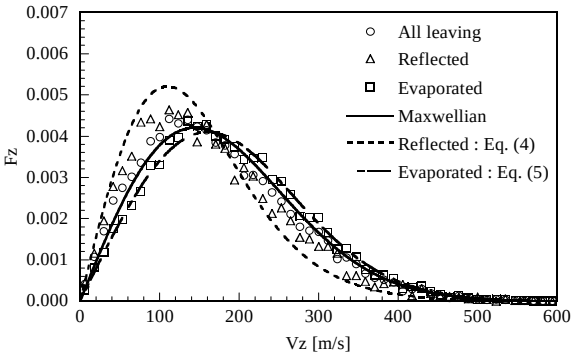

Figure 3 Velocity distributions in the vicinity of the condensing surface (130K-100K).

inverted temperature profile. Figure 2 shows the temperature profile in the vicinity of the condensing surface of our NEMD results. It is found that the inverted temperature profile occurs near the condensing surface under the non-equilibrium condition and the temperature jump at the liquid vapor interface (T^g-T^l) increases with the increasing of the temperature difference between the bulk vapor and bulk liquid. We have confirmed that the entropy production rate has a positive value in all simulation cases. Therefore, our NEMD results support the possible inverted temperature profile without any contradiction to the second law of thermodynamics[9].

On the other hand, we also find that the velocity distribution of the reflecting molecules obtained in our NEMD deviates from Eq. (4). This means that the reflecting molecules cannot accommodate to the liquid surface during the process of reflection in non-equilibrium conditions. This might be the main reason why the inverted temperature profile occurs and thus, it is a main topic in this paper.

NONEQUILIBRIUM MOLECULAR DYNAMICS STUDY

The nonequilibrium molecular dynamics (NEMD) simulation has been performed in a rectangle simulation box with the size of Lx=Ly=6.486nm and Lz=131.347nm as shown in Fig. 4. The length of the simulation cell in z direction corresponded to 30 times of the mean free path of argon gas at 100K. The periodic boundary conditions are utilized in the x, y and z directions. Total particle number in the system is 12000 and the technique of cell index method is used to improve the efficiency on calculations of force/potential field. The well-known Lennard-Jones potential function is applied to the force field of argon,

$$\phi_{ij}(r_{ij}) = 4\varepsilon\left\{\left(\frac{\sigma}{r_{ij}}\right)^{12} - \left(\frac{\sigma}{r_{ij}}\right)^{6}\right\} \qquad (6)$$

where, ϕ_{ij} is the potential energy between the pair of particles i and j of the intermolecular distance r_{ij}, σ= 0.3405nm is the diameter of argon, and ε is the potential parameter of ε/k_B=119.8K[19]. The velocity Verlet algorithm is used with the time step of Δt=5fs and the cutoff distance is set to 3.5σ.

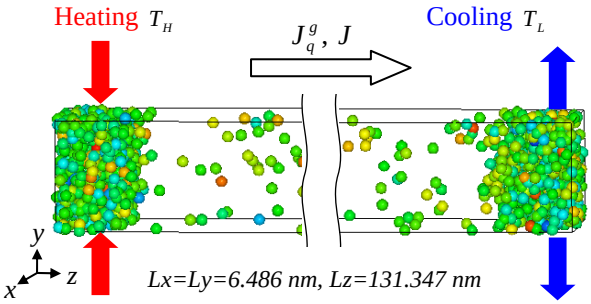

Figure 4 Non-equilibrium MD simulation system.

In order to maintain the nonequilibrium condition, two thermostats at different temperatures are prepared. The hot one is set in the liquid near the left end of the simulation cell and the cold one is at the right side. The thickness of the thermostat layer is 3.5σ. Therefore, the evaporation takes place at the left liquid-vapor interface and the condensation takes place at the right side. The cell is divided into 110 layers for the local data sampling of temperature and density. The pressure profile is obtained by solving the following equation using Irving-Kirkwood method[20].

$$P = \frac{1}{V}\left[\sum_{i}^{\beta} m_i\left[v_i - u_i\right]\left[v_i - u_i\right] + \frac{1}{2}\sum_{ij}^{\beta} r_{ij}F_{ij}\right] \qquad (7)$$

ACCOMMODATION COEFFICIENT FOR REFLECTING MOLECULES

Instead of the conventional accommodation coefficient, a new definition of the energy accommodation coefficient for the reflecting molecules is proposed:

$$\gamma = \frac{E_i - E_r}{E_i - E_s} \tag{8}$$

$$E_s = \int_0^\infty \frac{1}{2} m v_z^2 F_{z,r} dv_z = \frac{1-\alpha+\alpha\beta/4}{1-\alpha+\alpha\beta/2} k_B T \tag{9}$$

where E_i is the incident energy of the reflecting molecule, E_r is the escape energy after reflection, and E_s is the energy of the reflecting molecules accommodate to the liquid surface completely. In most studies, E_s is obtained based on Maxwellian distribution. However, the energy of the reflecting molecules is lower than that based on the Maxwellian distribution. Therefore, E_s is defined to be the energy of the reflecting molecules in equilibrium condition based on Eq. (4). That is, the accommodation coefficient of energy for reflecting molecules is unity in the equilibrium cases. When the condensing surface temperature is 102K, E_s is evaluated to be $0.679 k_B T$ (α=0.923 and β=0.299 in T=102K).

The accommodation coefficient obtained in the present NEMD is shown in Fig. 5. The accommodation coefficient decreases as the mass flux J increases in the bulk vapor corresponding to various non-equilibrium conditions. When the mass flux is small, the accommodation coefficient is close to unity. However, in the case of J=1400kg/(m^{2}s), the accommodation coefficient is reduced to 0.55.

Table 1 is a summary of the NEMD results on mass flux and temperature jump at the condensing surface. T^v and T^g represent the bulk vapor phase temperature and the vapor phase temperature at the liquid-vapor interface, respectively. Both the mass flux and the temperature jump increase when the temperature difference between the evaporating surface and the condensing surface increases. This implies that the vapor temperature near the condensing surface increase due to the excess energy of reflecting molecules. Therefore, a modified molecular boundary condition for the reflecting molecules is proposed as follows.

$$F_{z,r} = \frac{1-\alpha+\alpha\beta\exp\left(-mV_z^{\,2}/(2k_B T')\right)}{1-\alpha+\alpha\beta/2} \times \left(\frac{m}{k_B T'}\right) V_z \exp\left(-\frac{mV_z^{\,2}}{2k_B T'}\right) \tag{10}$$

Here, T' is the modified temperature of the condensing surface given as a function of mass flux and accommodation coefficient.

The velocity distribution for the reflecting molecules modified by the accommodation coefficient is shown in Fig. 6 in the dashed line. The NEMD data agree with Eq. (10) well and thus we conclude that the accommodation coefficient play important role on the molecular boundary condition for the reflecting molecules.

Table 1 Heat and mass fluxes adjacent to condensing surface

$T_H - T_L$	T^v [K]	T^g [K]	J [kg/(m^{2}s)]	$\Delta T/T^g$ [-]
110-100	100.3	103.2	666.8	-0.0317
115-100	102.5	105.4	869.3	-0.0493
120-100	103.2	107.6	1133.6	-0.0646
125-100	103.9	109.0	1442.8	-0.0724
130-100	104.6	109.4	1740.3	-0.0692

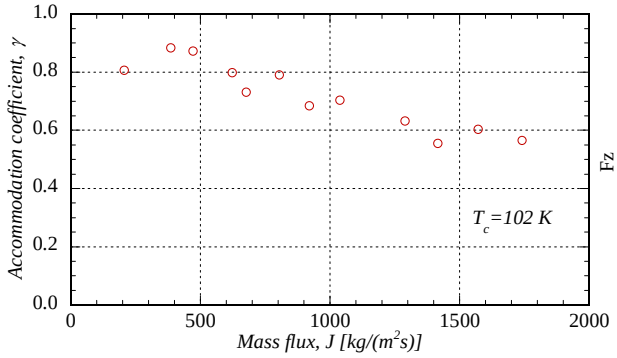

Figure 5 Accommodation coefficients by NEMD

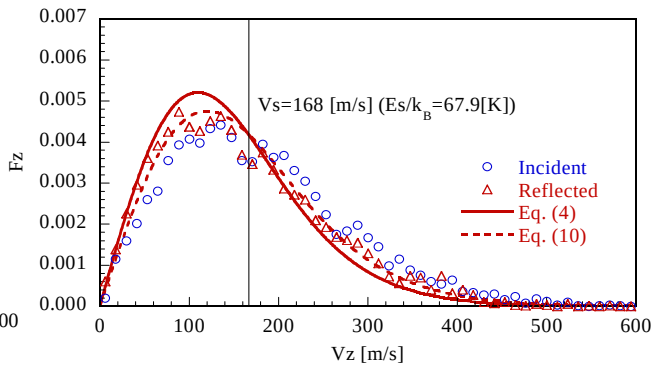

Figure 6 Velocity distribution of reflecting molecules

DIRECT SIMULATION OF MONTE CARLO METHOD

The DSMC analysis has been performed to verify the inverted temperature profile by applying the molecular boundary condition based on NEMD. The simulation system is shown in Fig. 7. One-dimensional condensing flow of argon vapor is considered. The bulk vapor phase is apart from the liquid surface in the distance of 30 times of the mean free path of argon gas at 100K. The simulation domain is divided into 90 cells and the number of sample molecules in a cell is about 1000. The condensing surface is in 102 K which is same to that of NEMD. For the collisions between the particles, the rigid sphere model and the maximum collision-number scheme are used. The time increment is about 10-times smaller than the mean free time and 100000 steps simulation period is performed to obtain the time-averaged results.

The simulation cases are summarized in Table 2. The pressure ratio of bulk vapor phase P_v to the surface saturation pressure P_C represents the non-equilibrium condition.

$$S = \frac{P_v}{P_c} \tag{11}$$

According to the kinetic theory, the mass flux from the bulk vapor phase to the condensing surface is expressed:

$$J = \zeta \frac{P_v - P_c}{\sqrt{2\pi R T_v}} = \frac{2\sigma_c}{2 - 0.798\sigma_c} \frac{P_v - P_c}{\sqrt{2\pi R T_v}} \tag{12}$$

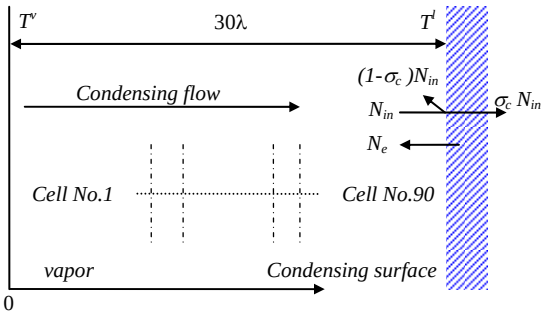

Figure 7 Simulation system and boundary conditions for DSMC analysis.

Here, ζ is given by Labuntsov based on the Schrage's expression in consideration of the non-equilibrium effect in the Knudsen layer adjacent to the liquid surface.

The temperature and pressure profile are shown in Figs. 8 and 9. The dimensionless temperature and pressure are defined as follows.

$$\theta = \frac{T - T_c}{T_v - T_c} \tag{13}$$

$$\Pi = \frac{P - P_c}{P_{sat}(T_v) - P_c}. \tag{14}$$

Table 2 Simulation cases of DSMC analysis. (T_c=102[K], P_c=0.3838[MPa])

ΔT [K]	$S=P_v/P_c$	J [kg/(m^{2}s)]	γ
3	1.232	314.2	1.00
3	1.232	314.7	0.90
3	2.165	1684.8	1.00
3	2.165	1684.8	0.55

As shown in Fig. 8, the temperature of both the cases of NEMD (S=2.165) and DSMC (S=2.165) increases near the condensing surface, which results in a negative gradient in the vapor phase. However, the normal temperature profiles are obtained in the DSMC simulation cases of S=1.232. This means that the inverted temperature profiles occurs easier in the strong condensation than the weak one. Simultaneously, it should be note that the accommodation coefficient is 0.55 for a given mass flux of J=1684.8 [kg/(m^{2}s)], while γ is 0.90 for the mass flux J=314.2 [kg/(m^{2}s)] (see Fig.

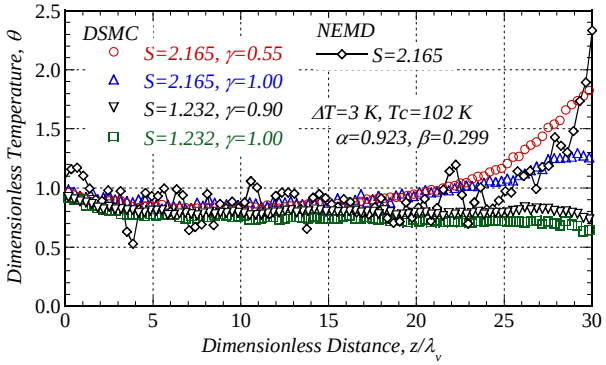

Figure 8 Temperature profiles

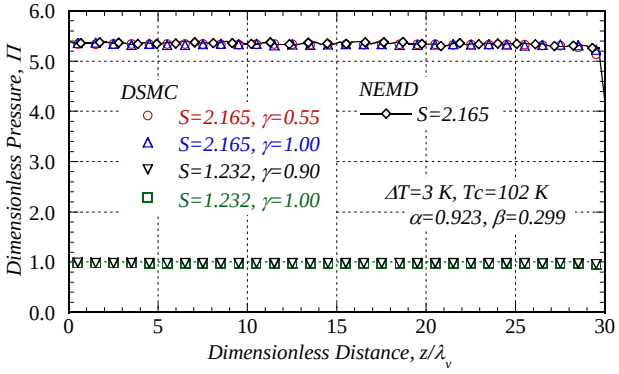

Figure 9 Pressure profiles

5). Comparing the DSMC results under the same condition of S=2.165, we can find that a larger temperature jump occurs in the case of γ =0.55 than that of γ =1.0. This implies that the inverted temperature profile occurs due to the excess energy of the reflecting molecules.

Figure 10 shows a comparison of the velocity distributions between the NEMD and DSMC results. The velocity distribution of the reflecting molecules of DSMC is in a good agreement with the nonequilibrium molecular boundary condition described by Eq. (10). The present molecular boundary condition including accommodation coefficient is appropriate to predict the mass transfer characteristics at the nonequilibrium liquid surface.

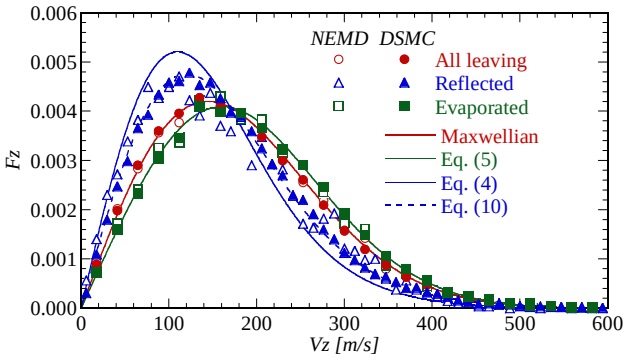

Figure 10 Velocity distributions.

CONCLUSION

A new molecular boundary condition for nonequilibrium liquid surface is proposed in this study. A new definition of the accommodation coefficient of energy for the reflecting molecules is introduced and its validity has been verified. The accommodation coefficient for the reflecting molecules decreased with the increasing of the mass flux in the vicinity of the liquid surface. The low accommodation coefficient for the reflecting molecules results in the accumulation of the excess energy at the liquid surface and this is the reason of the inverted temperature profiles.

REFERENCES

1. Tsuruta, T. et al., *International Journal of Heat and Mass Transfer* **42**, 4107-4116 (1999)
2. Tsuruta, T. and Nagayama, G., *Journal of Physical Chemistry B* **108**, 1736-1743 (2004)
3. Tsuruta, T. et al., *Transactions of the Japan Society of Mechanical Engineers, Series B* **64**, 456-462 (1998)
4. Pao, YP., *Physics of Fluids* **14**, 306-312 (1971)
5. Frezotti, A. et al., *Physics of Fluids* **15**, 2837-2842 (2003)
6. Meland, R., *Physics of Fluids* **15**, 3244-3247 (2003)
7. Bedeaux, D. et al., *Physica A* **169**, 263-280 (1990)
8. Kjelstrup, S. et al., *Journal of Colloid and Interface Science* **256** 451-461 (2002)
9. Tokunaga, A. et al., *in Proc. of the International Heat Transfer Conference*, Accepted, Washington, (2010)
10. Nagayama, G. and Tsuruta, T., *The Journal of Chemical Physics* **118**, 1392-1399 (2003)
11. Tsuruta, T. and Nagayama, G., *Energy* **30**, 795-805 (2005)
12. Sone, Y. and Onishi, Y., *Journal of the Physical Society of Japan* **44**, 1981-1994 (1978)
13. Aoki, K. and Cercignani, C., *Physics of Fluids* **26**, 1163-1164 (1983)
14. Hermans, LJF. and Beenakker, JJM., *Physics of Fluids* **29**, 4231-4232 (1986)
15. Ytrehus, T., *Multiphase Science and Technology* **9**, 205-327 (1997),
16. Shankar, P. and Deshpande, MD., *Physics of Fluids A-Fluid Dynamics* **2,** 1030-1038 (1990)
17. Fang, G. and Ward, CA., *Physical Review E* **59**, 417-428 (1999)
18. Johannessen, E. and Bedeaux, D., *Physics of Fluids* **19**, 017104-1-7 (2007)
19. Allen, MP. And Tildesley, DJ., Computer Simulation of Liquids (Clarendon, Oxford, 1987)
20. Irving, JH. and Kirkwood, JG., *Journal of Chemical Physics* **18**, 817-829 (1950)